Gap Modes due to Cl^- and Br^- in KI†

I. G. NOLT, R. A. WESTWIG,* R. W. ALEXANDER, JR., AND A. J. SIEVERS
Laboratory of Atomic and Solid State Physics, Cornell University, Ithaca, New York
(Received 19 December 1966)

Optically active lattice gap modes associated with Cl^- and Br^- substitutional impurities in KI have been studied. High-resolution far-infrared absorption measurements in KI:Cl^- at a temperature of 2°K have revealed an isotope frequency shift of 0.31 ± 0.05 cm^{-1}. The gap-mode center frequencies are 76.79 and 77.10 ± 0.05 cm^{-1} and are attributed to Cl^{37} and Cl^{35} impurities, respectively. The isotope frequency shift for the Br^--induced gap mode at 73.8 ± 0.10 cm^{-1} is not completely resolved, but an upper limit of 0.15 cm^{-1} is established on the basis of the observed linewidth. For both cases the small isotope shift can be qualitatively understood with a simple lattice model in which the perturbed nearest-neighbor force constant at the impurity site is less than the nearest-neighbor force constant of the unperturbed crystal. The temperature dependence of the absorption in KI:Cl^- also has been measured.

I. INTRODUCTION

THE infrared absorption spectrum associated with the vibrational motion of a small mass impurity in a crystal lattice was first observed in 1958.[1] At that time Schäfer measured the infrared transmission of a number of alkali halide crystals containing the hydride ion as a substitutional impurity and found a sharp absorption line at a frequency more than two times the maximum phonon frequency of the host lattice. The position of the absorption line was found to depend on the lattice spacing of the host crystal. On replacing the hydride-ion impurity by the deuteride ion, an isotope shift of approximately $\sqrt{2}$ was observed.[1,2] Weak absorption bands also were found near the principal lattice absorption line. In recent years the investigation of the sideband structure[3,4] has yielded a wealth of detailed information on the mechanics of the impurity-lattice coupling, but to date only the hydride-ion impurity has been observed to produce infrared-active localized lattice modes at frequencies which are higher than the maximum phonon frequency of the host lattice. In contrast with the experimental situation for high-frequency local modes, lower-frequency localized lattice modes have been observed for a variety of impurities at frequencies in the gap region between the optic and acoustic phonon branches in potassium iodide.[5]

Mazur *et al.*[6] first calculated the properties of gap modes for a simple diatomic linear chain model with an isotopic impurity replacing either the light or the heavy mass of the diatomic chain. For some impurity-mass–lattice-mass combinations, both infrared-active localized lattice modes above the top of the phonon spectrum as well as gap modes are possible. With a more realistic three-dimensional lattice model a quantitative comparison of theory and experiment already has been attempted for the experimentally observed gap mode at 77 cm^{-1} in KI:Cl^-.[7] The Cl^- substitutional impurity has been treated as a mass defect and the gap- and resonant-mode frequencies have been calculated for the potassium iodide host crystal. The calculation of the eigenfrequencies and eigenvectors of the perfect lattice was based on Hardy's deformation dipole model[8] of ionic crystals which gave a gap in the frequency spectrum of KI from 64.1 to 79.4 cm^{-1}. Although good agreement between theory and experiment for the eigenfrequency of the gap mode was obtained, the recent measurement of the normal-mode spectrum of KI by Dolling *et al.*[9] using inelastic neutron scattering shows that the gap extends from 69.7 to 95.6 cm^{-1}. It is now evident that the Cl^- gap mode in KI cannot be described with a simple mass defect.

In order to clarify the experimental situation we have made additional measurements of the far-infrared absorption induced by Cl^- and also Br^- ions in KI at low temperatures. With an instrumental resolution of 0.21 cm^{-1}, the induced absorption previously reported at 77 cm^{-1} has been resolved into a doublet with components separated by 0.31 cm^{-1}. The strength of the doublet is temperature-independent from 2 to 10°K and the two lines are attributed to the naturally occurring isotopic mixture of mass-37 and mass-35 chloride ions. The isotope shift for the Br^- impurity absorption is less than 0.15 cm^{-1} and is not completely resolved. For both impurities the gap-mode frequencies and small isotope shifts can be understood with a simple lattice model in which the perturbed nearest-neighbor force

† Work supported by the U. S. Atomic Energy Commission. Additional support received from the Advanced Research Projects Agency through the use of central facilities and space provided by the Materials Science Center.

* Present address: Corning Glass Works, Corning, New York.

[1] G. Schäfer, J. Phys. Chem. Solids **12**, 233 (1960).

[2] W. C. Price and G. R. Wilkinson, University of London, King's College, Molecular and Solid State Spectroscopy Technical Report No. 2, 1960 (unpublished).

[3] B. Fritz, in *Proceedings of the International Conference on Lattice Dynamics, Copenhagen, 1963*, edited by R. F. Wallis (Pergamon Press, Inc., New York, 1965).

[4] T. Timusk and M. V. Klein, Phys. Rev. **141**, 664 (1966).

[5] A. J. Sievers, in *Low Temperature Physics* edited by J. G. Daunt *et al.* (Plenum Press, Inc., New York, 1965), Vol. LT9, Part B.

[6] P. Mazur, E. W. Montroll, and R. B. Potts, J. Wash. Acad. Sci. **46**, 2 (1956).

[7] A. J. Sievers, A. A. Maradudin, and S. S. Jaswal, Phys. Rev. **138**, A272 (1965).

[8] A. M. Karo and J. R. Hardy, Phys. Rev. **129**, 2024 (1963).

[9] G. Dolling, R. A. Cowley, C. Schittenhelm, and I. M. Thorson, Phys. Rev. **147**, 577 (1966).

constant at the impurity site is less than the nearest-neighbor force constant for the unperturbed crystal.

In the next section the experimental apparatus and measurements are described. The experimental results for the chlorine- and bromine-induced gap modes are presented in Sec. III. Finally, in Sec. IV, the experimental results are qualitatively interpreted with a simple lattice model.

II. EXPERIMENTAL APPARATUS

The impurity-induced absorption spectra have been measured over the frequency interval from 4 to 100 cm^{-1}. Both a grating monochromator and a lamellar interferometer have been used in the range from 45 to 100 cm^{-1}. Below 45 cm^{-1} the interferometer has been employed exclusively.

The grating monochromator is an $f/1.5$ Ebert-Fastie system of our own construction.[10] The optical system, shown in Fig. 1, is contained in a vacuum tank formed by two standard steel bell jars. The source S is a GE UA-2 mercury arc lamp with its output chopped at a frequency from 10 to 50 cps by a slotted metal disk for synchronous detection. The variable chopping frequency, which allows optimization of the detector response, is obtained by using a signal generator and a power amplifier to power the synchronous chopping motor. In Fig. 1, the filter gratings used in zero order at F1 and F2 and a 0.1 mm film of carbon-filled polyethylene in the baffle window remove most of the high-frequency radiation from the beam. M1 and M4 are aluminum off-axis ellipsoidal reflectors with the extended source aberrations reduced by the Czerny-Turner type of arrangement.[11] The final image of unit magnification after $M5$ is channeled to the entrance slit by a 1.25-cm-diam light pipe 8 cm long. The collimating mirror $M6$ is an aluminized Pyrex parabola 35 cm in diam with a focal length of 45 cm. A brass light pipe is again used to conduct the radiation from the exit slit to the cryostat.

For the frequency range from 45 to 100 cm^{-1}, a grating, labeled G in Fig. 1, with a blazed ruling of 254 μ and filter gratings, F1 and F2, of 80 μ spacing were used. No transmission filter, F3, was used for this frequency interval, but instead a low-temperature (4°K) transmission filter consisting of layers of crystal quartz, KCl, NaCl, KBr, and carbon-filled polyethylene was placed in the cryostat light pipe. The sensitivity of our detector placed a practical limit of about 75 on the instrumental resolving power for the single-pass arrangement with a 10-sec-integrating time. Higher resolution was achieved with a double-pass design, not shown in Fig. 1, which used a Walsh-type[10,12] reimaging mirror placed symmetrically with respect to the entrance and exit slits in the focal plane of the collimating parabola. The resulting second reflection from the grating doubled the dispersion, and, under the conditions of energy-limited resolution, this was a more efficient method for increasing the resolution than slit-width reduction.[10] With this modification we readily achieved a resolving power of 150.

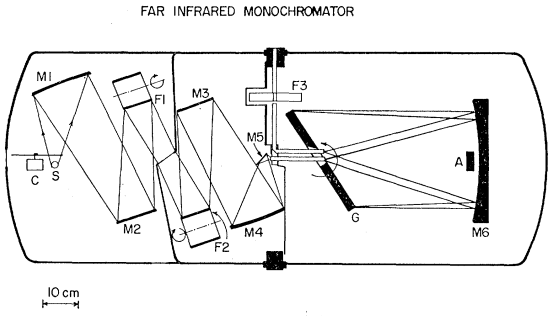

FIG. 1. Optical system of the far-infrared grating spectrometer in single-pass (top view). The instrument is an $f/1.5$ Ebert-Fastie on-axis design enclosed in a vacuum tank. The optical path is indicated by the arrows. S is the Hg arc source chopped by a slotted disk chopper C. M designations refer to mirror components. F1 and F2 are zero-order reflection gratings and F3 is a transmission-type filter. A is an absorber for preventing direct reflection to the exit slit. G is the grating.

All measurements of absorption as a function of impurity content were made with the grating instrument. The investigation of the finer details of the spectra required higher-resolution measurements than were possible with our grating monochromator. For these measurements we have used a Strong-type interferometer.[10,13,14] This instrument utilizes the same optical system described above with the grating G replaced by the lamellar assembly. The lamellar grating is composed of two sets of interleaving aluminum plates forming a reflecting surface consisting of parallel grooves 1.2-cm wide. The groove depth is varied from zero to some maximum value in an incremental fashion by a micrometer lead screw. The collimated beam incident on the lamellar surface is thus divided by "wavefront division" into two interfering components with an optical path difference Δ equal to twice the groove depth. The resultant zero-order energy is focused on the exit slit and channeled to the sample and detector cryostat by a 1.25-cm-diam light pipe. The bolometer signal measured as a function of the groove depth $\Delta/2$ is automatically recorded on punch cards and comprises the interferogram $I(\Delta)$ of the transmitted spectral distribution $S(\nu)$.

The transmission spectrum $S(\nu)$ is related to $I(\Delta)$ by a Fourier transform. Because the first datum point is adjusted to the position of zero path difference, only the cosine transform need be considered. This spectrum,

[10] I. G. Nolt and A. J. Sievers, J. Opt. Soc. Am. **55**, 1586 (1965); and (to be published).
[11] M. Czerny and A. F. Turner, Z. Physik **61**, 792 (1930).
[12] A. Walsh, J. Opt. Soc. Am. **42**, 195 (1952).
[13] J. Strong and G. A. Vanasse, J. Opt. Soc. Am. **50**, 113 (1960). For an up-to-date synopsis of interferometry with an excellent set of references see E. V. Lowenstein, Appl. Opt. **5**, 845 (1966).
[14] P. L. Richards, J. Opt. Soc. Am. **54**, 1474 (1964).

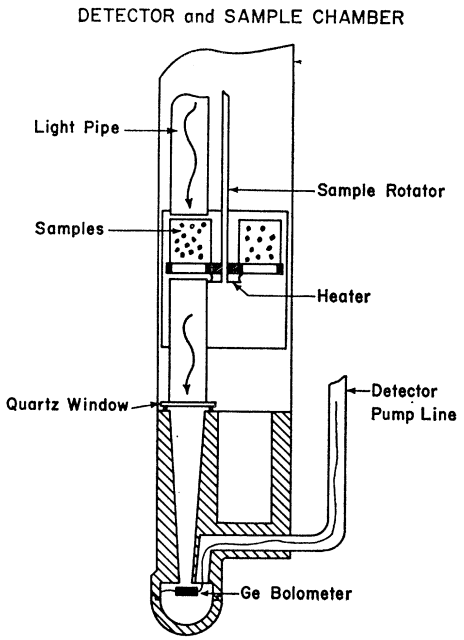

FIG. 2. Schematic cross section of the liquid-helium-immersed sample cryostat used for temperature-dependence measurements. Sample temperatures from 2 to 35°K can be obtained with this system. A 1000-Ω carbon resistor (not shown) attached to the sample is usually employed to determine sample temperature.

which is calculated on a digital computer, is given by

$$S(\nu=m\nu_1)=\frac{I(0)}{2}+2\sum_{n=1}^{N}\left[I(nh)-\frac{I(0)}{2}\right]\times\left(1-\frac{n}{N}\right)\cos\left(\frac{\pi nm}{N}\right), \quad (1)$$

where $N+1$ equals the total number of values for $I(\Delta)$, h is twice the increment in groove depth, ν_1 is given by $1/2Nh$,[15] and $I(nh)$ is the measured intensity at Δ equal to (nh). The quantity $(1-n/N)$ is the triangular apodization term which serves to reduce the magnitude of the side bands on the instrumental slit function at the sacrifice of some resolution.[14] Both unapodized and triangularly apodized transmission spectra were calculated, but the absorption coefficient is based on the apodized results in all cases. We evaluated the above expression using the computational method devised by Cooley and Tukey.[16] For high-resolution measurements over a wide spectral range, the time saved by this method, as pointed out by Forman,[17] becomes appreciable. The complete inversion of a typical interferogram consisting of 1000 points, including all the peripheral calculations, required 3 min on a CDC 1604.

[15] This expression needs to be corrected slightly for the nonnormal incidence of the radiation upon the lamellar surface. Taking this into account, ν_1 is given by 1.00071/2Nh.

[16] J. W. Cooley and J. W. Tukey, Math. Computation **19**, 296 (1965).

[17] M. L. Forman, J. Opt. Soc. Am. **56**, 978 (1966).

The calculated spectrum extends up to a cutoff frequency ν_c given by $1/2h$. The increment h was 0.005 cm for a frequency cutoff of 100 cm^{-1}. It is essential that radiation at frequencies above the value ν_c be filtered from the beam. This is accomplished by the same filtering scheme described previously. The instrumental resolution for the apodized calculation of the absorption coefficient is given to a good approximation by $1/Nh$, where Nh is simply twice the maximum groove depth. The resolution and frequency calibration were checked by the measurement of water vapor absorption in the air gap of about $\frac{1}{2}$ cm separating the spectrometer and cryostat light-pipe flanges. The water-vapor doublet at 55 cm^{-1} with a separation of 0.29 cm^{-1} [14] was of particular interest, since its splitting approximated the chlorine-isotope splitting which is described in Sec. III. These frequency comparisons agreed well within a precision of 0.05 cm^{-1}.

In this study, where both grating and interferometric techniques were used and compared, interferometric spectroscopy was found to be the most practical means for achieving high-resolution spectra in the far infrared, in contrast with the conclusion of Kneubühl *et al.*[18]

The far-infrared radiation was detected with a liquid-helium-cooled gallium-doped germanium bolometer which was assembled by one of the authors (R.A.W).[19] Figure 2 shows the arrangement of the sample and detector assembly in the low-temperature cryostat. This system is immersed in a pumped-liquid-helium bath at a temperature of 1.3°K. The $f/1.5$ radiation beam is reflected down a gold-plated stainless-steel light pipe, and passes through the transmission filter (not shown), the sample, a crystal-quartz vacuum-

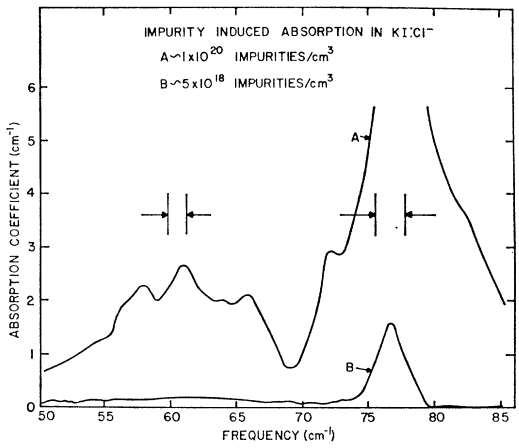

FIG. 3. Cl^--induced absorption in KI. The absorption coefficient relative to an undoped KI sample is shown as a function of frequency. The impurity content of the specimens is given in Table I. These measurements have been made using the grating monochromator in single pass with the instrumental resolution indicated by the frequency intervals between the arrows.

[18] F. K. Kneubühl, J. F. Moser, and H. Steffen, J. Opt. Soc. Am. **56**, 760 (1966).

[19] R. A. Westwig, M.S. thesis, Cornell University, 1967 (unpublished); F. J. Low, J. Opt. Soc. Am. **51**, 1300 (1960).

tight window, and a condensing cone into the nonresonant copper cavity containing the bolometer. Four samples plus a resistance heater and thermometer are mounted on the sample ring which is rotated from outside the cryostat to position the desired sample in the beam. The crystal-quartz window isolates the sample chamber from the detector cavity. In this way the helium exchange gas which is required to cool the samples to the bath temperature does not affect the detector sensitivity. The exchange gas can be removed and the samples then heated with a resistance heater. Temperatures up to 35°K can be obtained without appreciably influencing the detector sensitivity. A 1000-Ω Allen-Bradley resistor served as the resistance thermometer. During the temperature-dependent runs, the resistance was continuously monitored by a 25-cps bridge having a power dissipation of less than 10^{-8} W. Manual adjustment of the heater current held the sample temperature constant to within ±1°K up to 15°K. Also, with the cryostat arrangement shown in Fig. 2, the sample can assembly may be withdrawn from the cryostat and the samples changed while the detector remains at 4.2°K.

III. EXPERIMENTAL RESULTS

A. Cl^--Induced Gap Modes

The experiments reported here pertain to the chloride-induced far-infrared absorption as a function of impurity concentration, isotopic Cl^- mass, and temperature. KI single crystals with four different concentrations of chloride ions were grown by the Kyroupolos method in an argon atmosphere. The impurity-induced absorption spectrum was determined for all the samples at 2°K. We used the grating monochromator, described previously, in a single-pass mode with a resolving power of about 40. Figure 3 shows the absorption coefficient obtained by comparing the transmission of the doped sample to that of an undoped KI crystal for the highest and lowest concentrations of the four boules. The main feature is the strong absorption line at 77 cm^{-1}. No impurity-induced absorption has been found below 30 cm^{-1}.[20] The shoulder at 74 cm^{-1} has been identified with the presence of an unwanted bromide impurity. This absorption line arises from the Br^- gap mode which will be considered in more detail in the following section.

The area under the four chlorine-induced absorption lines, which we shall call the line strength, is found to vary linearly with the chemically determined Cl^- concentration. The linear dependence leads us to define an oscillator strength f for the absorption lines in analogy with the strength defined for electronic transitions. The

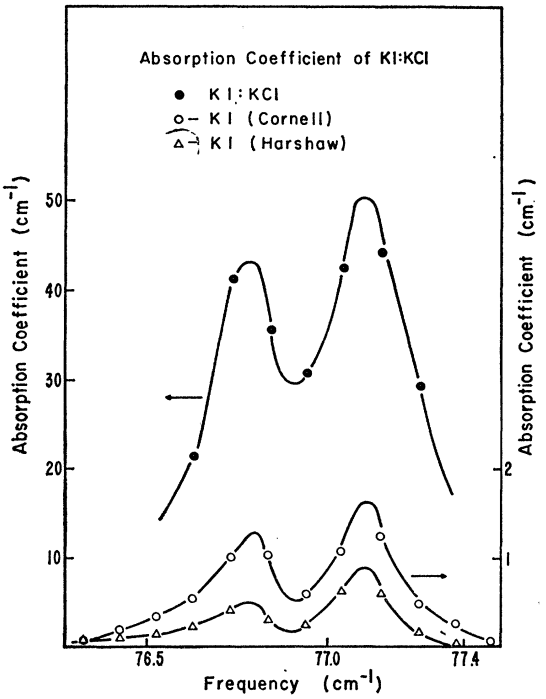

FIG. 4. Gap-mode absorption in KI:Cl^- between 76.5 and 77.4 cm^{-1}. Note different left and right ordinate scales. This figure shows the isotope frequency shift due to chloride impurities of mass-35 and mass-37 in their natural abundance ratio of approximately 3:1. The KI:KCl sample was from the same boule as sample B in Fig. 3. These measurements were obtained using the interferometer described in the text with a resolution bandwidth of 0.21 cm^{-1}.

oscillator strength f is calculated from the relation[21,22]

$$\int \alpha(\nu)d\nu = \frac{e^2}{(\sqrt{\epsilon_0})c^2M^*}\left[\frac{\epsilon_0+2}{3}\right]^2 Nf, \qquad (2)$$

where ϵ_0 is the dielectric constant of the host crystal at the local mode frequency, e is the electronic charge, M^* is the effective mass, and N is the number of impurities per cm^3. For the four absorption lines ascribed to the chlorine impurity we find the oscillator strength $f=0.03$. For the sharp line at 77 cm^{-1} alone, $f=0.016$.

Because the phonon gap between the acoustic and optic branches in KI extends from 69.7 to 96.5 cm^{-1}, the three broad absorptions centered at 58, 61, and 66 cm^{-1} occur in the acoustic-phonon spectrum. We shall see in the next section that similar peaks occur at 56, 61, and 67 cm^{-1} in KI:Br^-. In neither case do the absorption peaks seem to identify critical points in the KI density-of-modes spectrum. However, such frequency shifts are to be expected for the two impurities if the absorption lines are to be identified with resonant or incipient resonant modes which occur in

[20] We have looked for lattice resonant absorptions in KI:LiCl. Even for very highly doped samples no absorptions attributable to either Li^+ or Cl^- have been observed over the range from 3 to 30 cm^{-1}.

[21] D. J. Dexter, Phys. Rev. **101**, 48 (1956); W. T. Doyle, *ibid.* **111**, 1072 (1958).

[22] P. G. Dawber and R. J. Elliott, Proc. Phys. Soc. (London) **81**, 453 (1963).

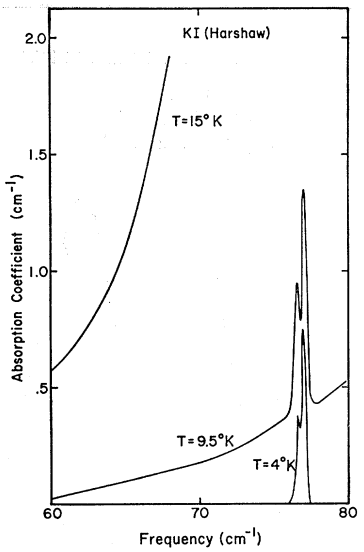

FIG. 5. Infrared absorption in the nominally pure Harshaw sample (see Table I) between 60 and 80 cm^{-1} as a function of sample temperature. The sharp absorption at 77 cm^{-1} is due to an intrinsic Cl^- impurity content of about 0.5×10^{16} ions/cm^3. Above 10°K the rapidly increasing background absorption due to phonon difference band processes in the host crystal mask the gap mode at 77 cm^{-1}.

the frequency region of the large density of modes. A satisfactory method for investigating the nature of these broad resonant modes has not yet been found and we now turn to the study of the gap-mode absorption at 77 cm^{-1}.

In Fig. 3 the line at 77 cm^{-1} is still quite prominant in the lightly doped sample B after most evidence of the broad lines has disappeared. The resolution of the grating instrument is insufficient to resolve the gap-mode linewidth; consequently, the absorption spectrum of the same sample B has been remeasured using the interferometer with a resolution bandwidth of 0.21 cm^{-1}. Figure 4 shows the resultant spectrum for sample B as well as for two additional nominally pure KI samples. The absorption coefficient over the small frequency region shown here has been determined by comparing the transmission of the alkali halide to that of crystal quartz normalized to have the same transmission adjacent to the absorption line. At this higher resolving power of $\nu/\Delta\nu=380$, the gap mode at 77 cm^{-1} is found to consist of two lines with center frequencies of 77.10 and 76.79 ± 0.05 cm^{-1}. The frequency separation is estimated to be 0.31 ± 0.05 cm^{-1}. The two pure samples show a similar but much weaker doublet, although the sample thickness is over twenty times that of the KI:KCl sample. On the basis of the previously computed oscillator-strength value, the absorption strength of the two nominally pure samples corresponds to a chloride concentration of 5×10^{16} to 1.0×10^{17} Cl^-/cm^3. A close study of the absorption doublet indicates that the center frequencies and linewidths do not change noticeably, although the chloride concentration changes by a factor of ~100. For all three concentrations the line shapes appear to be asymmetric. This asymmetry does not appear to be an instrumental problem because it has not appeared in any of the several water-vapor spectra which were used to check our calibration. Taking the asymmetry into account, the relative ratio of the line strengths for the doublet components is about 3 to 1. We conclude that the doublet absorption in both the chloride-doped and also the nominally pure crystals arises from the presence of the two stable chlorine isotopes, 35 and 37, in their natural abundance ratio of approximately 3 to 1.[23]

The temperature dependence of the chloride-induced gap-mode doublet has been measured from 2 to 15°K with an interferometer resolution of 0.21 cm^{-1}. The absorption of the Harshaw sample compared to that of crystal quartz, adjusted for the difference in reflectivities, is shown in Fig. 5 for sample temperatures of 4, 9.5, and 15°K. As the temperature is increased, the sharp doublet does not change appreciably, except to appear on a broad background absorption. The background absorption has become strong enough by a temperature of 15°K, to control the absorption in this frequency region. Excluding this temperature-dependent background, the strength and width of the doublet is constant within our experimental precision over this temperature range.

The broad temperature-dependent absorption in this frequency region is due to the anharmonic coupling of the transverse optic phonons with two other lattice phonons.[24,25] The absorption of a photon creates one phonon and destroys a lower-energy phonon giving rise to a "difference" band. The absorption coefficient for this process varies as the difference in population of the two phonon modes. Using the known density of phonon modes for KI, Lytle has demonstrated that such a temperature dependence is observed for the gap region.[26]

Recently, Renk, with a resolution quite a bit better than Lytle's, reported a sharp temperature-dependent line at 77 cm^{-1} which he attributed to the same difference-band process.[27] The results illustrated in Fig. 5 show no such temperature dependence of the sharp line over the same temperature region studied by Renk. The absence of a strong temperature dependence for the narrow doublet is consistent with the Cl^- gap-mode assignment. The temperature dependence of the broad background absorption, on the other hand, is consistent

[23] A mass-spectrograph analysis of the "Cornell" sample by the Analytical Chemistry Facility of the Materials Science Center of Cornell University indicated an abundance ratio in agreement with the expected value of 75.4% Cl^{35} and 24.6% Cl^{37} (*Handbook of Chemistry and Physics*, edited by C. D. Hodgman, Chemical Rubber Publishing Company, Cleveland, 1957), 39th ed.

[24] E. Burstein, *Phonons and Phonon Interactions*, edited by T. A. Bak (W. A. Benjamin Inc., New York, 1964), p. 276.

[25] R. Stolen and K. Dransfeld, Phys. Rev. **139**, A1295 (1965).

[26] C. D. Lytle, M. S. thesis, Cornell University, Materials Science Center Report No. 390, 1965 (unpublished).

[27] K. F. Renk, Phys. Letters **20**, 137 (1966).

with the results and interpretation by Lytle in terms of phonon difference bands.

B. Br⁻-Induced Gap Modes

The activation of gap modes by bromide impurities in KI has also been studied. Four single-crystal samples containing 6×10^{18} to 2×10^{21} Br^-/cm^3 were grown in air by the Kyroupolos method from untreated salts. The absorption spectrum for the sample containing 7×10^{19} Br^-/cm^3 relative to that of an undoped sample is shown in Fig. 6 (also, see Table I). Transmission measurements down to 4 cm^{-1} revealed no low-frequency absorption lines. An absorption spectrum very similar to that found previously for the chloride doping is observed; namely, three fairly broad absorption bands below the acoustic edge at 56, 61, and 67 cm^{-1}, plus a sharp line at 73.8 cm^{-1}. The line at 77 cm^{-1} is attributed to an unwanted Cl^- impurity which a chemical analysis showed to be present in this crystal in a concentration of 3×10^{18} Cl^-/cm^3. The spectrum shown in Fig. 6 has been obtained using the grating monochromator in a double-pass mode. For Br^- concentrations of less than 2×10^{20} Br^-/cm^3, the impurity-induced absorption strength, excluding the chlorine line, scales with the measured Br^- concentration. For the three broad bands plus the sharp line, the oscillator strength $f=0.016$. For the sharp line alone, $f=0.004$.

The gap mode at 73.8 cm^{-1} should also show an isotope shift, because Br^- is composed of very nearly equal mixtures of isotope 79 and isotope 81. We sought to detect the isotope effect; however, a resolution of 0.21 cm^{-1} is insufficient to resolve the frequency difference. An upper limit on the isotope shift can be obtained from the total linewidth, measured to be 0.45 cm^{-1}, composed of the absorption plus the instrumental contribution. If these gap modes have widths comparable with the Cl^- lines, the isotope shift is $\lesssim 0.15$ cm^{-1}.

IV. DISCUSSION OF EXPERIMENTAL RESULTS

The experimental results for the Cl^- and Br^- gap modes will now be compared with a simple lattice model described by Mitani and Takeno (hereafter referred to as MT).[28] They have calculated the frequencies of the gap modes for a lattice system consisting of a point defect with mass and nearest-neighbor force constants taken to be different from those of the NaCl-type host lattice. The long-range interaction forces which introduce coupling between the components of motion, as well as polarizability effects and lattice distortion, are not considered in this model. With the lattice coupling confined to nearest neighbors only and central and noncentral force constants set equal to each other, a solution for the eigenfrequency of the infrared-active gap mode is found which is particularly easy to handle. Only the knowledge of the nearest-neighbor spring constant K and the mass ratio M_1/M_2 of the host atoms (or equivalently, the frequencies of the top of the acoustic branch ω_1 and the bottom of the optic branch ω_2) are required to determine the eigenfrequencies and eigenvectors of the host crystal. In order to correct for some of the obvious deficiences of this simple model we use the mass ratio as a parameter and ω_1 and ω_2 are chosen to correspond to the measured phonon gap for KI.[9] The details of the determination of the infrared-active gap-mode frequency are deferred to Appendix I and only the general form of the equation which gives the eigenfrequency is presented here. A close analogy with the previously treated mass-defect problem[7] can be maintained if the expression is written as

$$y^2B(y)=1/\epsilon^*, \tag{3}$$

where $y=\omega/\omega_1$ is the normalized frequency and ω_1 is the maximum acoustic-mode frequency of the host lattice. The quantities $B(y)$ and $1/\epsilon^*$ are defined in Appendix I by Eqs. (A6) and (A7), respectively. $B(y)$ is a fairly complicated expression but depends only on

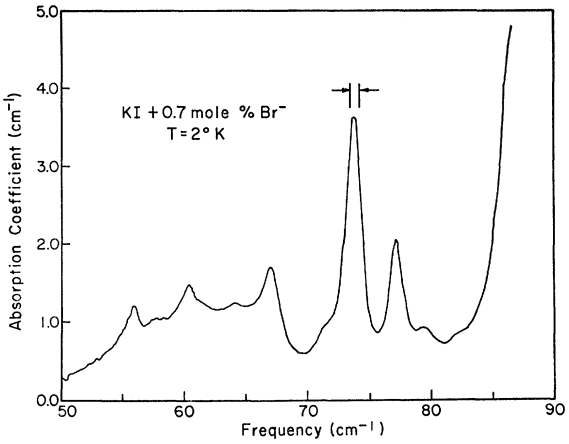

FIG. 6. Br^--induced absorption in KI. The sample shown here was grown from untreated salt and a chemical analysis indicated 7×10^{19} Br^-/cm^3 plus an unwanted chloride impurity of 3×10^{18} Cl^-/cm^3. The Br^--induced gap-mode absorption has a center frequency of 73.8 cm^{-1}. The line at 77 cm^{-1} is due to the chloride impurity. The instrumental resolution is indicated by the arrows.

TABLE I. Bromide and chloride concentrations in the KI samples.

Sample identification	Analyzed dopant content[a] (ions/cm³)	Other impurity content (ions/cm³)
A	1×10^{20} Cl^-	not measured
B	5×10^{18} Cl^-	not measured
KI (Cornell)	···	1.0×10^{17} Cl^-[b]
KI (Harshaw)[c]	···	0.5×10^{17} Cl^-[b]
KI+0.7 mole% Br^-	7×10^{19} Br^-	3×10^{18} Cl^-

[a] Chloride and bromide contents were measured by the Analytical Laboratory of the Materials Science Center at Cornell University.
[b] The concentration is estimated from the oscillator strength given in the text of this report.
[c] The KI sample was obtained from Harshaw Chemical Company, Cleveland, Ohio.

[28] Y. Mitani and S. Takeno, Progr. Theoret. Phys. (Kyoto) 33, 779 (1965).

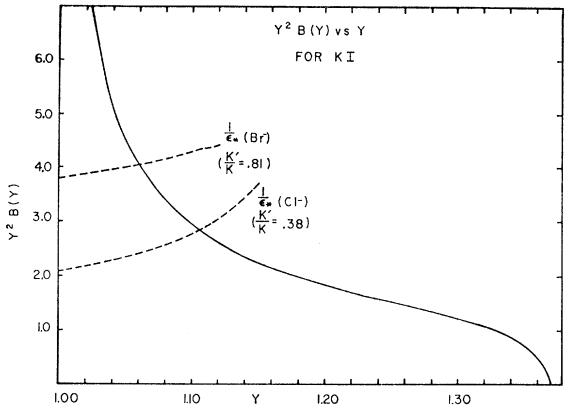

FIG. 7. A plot of $y^2B(y)$ for the gap frequency range in KI. $y=\omega/\omega_1$, where ω_1 is the maximum acoustic-branch frequency in KI(69.7 cm^{-1}). $B(y)$ is defined by Eq. (A7). The dashed curves represent the function $1/\epsilon^*$ defined by Eq. (A6). The intersection where $y^2B(y)=1/\epsilon^*$ gives the frequency of the infrared active gap mode.

the details of the host crystal. $1/\epsilon^*$ contains the information about the impurity ion, that is, the mass defect M'/M and the force-constant change K'/K. Using the experimental values for ω_1 and ω_2 for KI, the function $y^2B(y)$ for the gap region is shown in Fig. 7. The intersection of $1/\epsilon^*$ with $y^2B(y)$ yields the gap-mode frequency, as illustrated in Fig. 7, for the Cl^- and Br^- impurities. Taking the impurity mass to be the atomic mass, $K'/K=0.38$ gives an impurity-mode frequency of 77 cm^{-1} for the Cl^- ion and, similarly, $K'/K=0.81$ for the Br^- ion. Thus, the MT model gives the appropriate gap-mode frequencies for values of $K'/K<1$. The internal consistancy of these fits can be checked with the isotope-shift data. For Cl^- with $K'/K=0.38$, the shift in frequency associated with the chloride-mass change is calculated to be 1.74 cm^{-1} compared to the measured value of 0.31 cm^{-1}. With $K'/K=0.81$ for the Br^- impurity, the model predicts an isotope shift of 0.26 cm^{-1}, while the experimental shift is less than 0.15 cm^{-1}. The isotope shift appears to be a sensitive function of the impurity coupling constants. For both impurities, the model fails to account for the small isotope shift observed, although the calculated shifts are, indeed, much less than the maximum possible shift given by the square root of the isotope-mass ratio. Qualitatively, the model accounts for both the gap-mode frequency and the isotope shift with a small coupling constant. (For example, for the Cl^- impurity $K'/K=0.38$ gives the experimentally observed gap-mode frequency and $K'/K=0.5$ gives the observed isotope shift of 0.31 cm^{-1}.) Soft coupling to the lattice might have been expected intuitively because both impurity ions are smaller than the host ion they replace. In fact, if we assume that the impurity-ion diameter scales with the lattice constant a_0 of the corresponding potassium halide, then $a_0(KCl)<a_0(KBr)<a_0(KI)$ and, from the model, $K'(Cl^-)<K'(Br^-)<K(I^-)$.

The MT model defines K' as the nearest-neighbor force constant, but it is probably more meaningful to consider it as an effective nearest-neighbor coupling constant. In this way polarization effects in the lattice could be included to some extent. The importance of the electronic polarization on the effective coupling constant has been demonstrated by Matthew.[29] With a simple one-dimensional model, he showed that the electronic dipoles which arise from distortion of the ion cores act in such a manner as to destabilize the impurity ion. For our simple model, then, the effective coupling constant depends on the difference between the repulsive interaction and the polarization interaction. Since only the difference is important, neither term need be small to produce a soft coupling between the impurity and the lattice.

V. SUMMARY

In some cases impurity-induced absorption in KI crystals can be studied with far-infrared spectroscopic techniques. Whereas only the H^- local mode appears above the phonon spectrum of the pure crystal, a number of gap modes between the optic- and acoustic-phonon branches have been observed. These gap modes are extremely sharp, with full absorption linewidths at one-half the maximum absorption which are less than 0.21 cm^{-1}. Only limited temperature-dependence studies have been possible because of the intrinsic phonon absorption band from the host crystal. An isotope shift has been measured for the Cl^- isotopes and the shift appears to be a sensitive probe of the impurity-lattice coupling. The gap-mode frequency and isotope shift can be qualitatively understood with a simple lattice model in which the impurity ion is weakly coupled to the lattice.

ACKNOWLEDGMENTS

We thank Professor S. Takeno for his close cooperation on some of the theoretical problems. Also, discussions with Professor J. A. Krumhansl, Professor R. O. Pohl, and Professor A. A. Maradudin have been particularly helpful.

APPENDIX I

A particular example of a defect lattice system which has been treated in detail is the simple cubic lattice with a substitutional impurity.[30] The lattice consists of point masses coupled to nearest neighbors with harmonic springs. The nearest-neighbor force constant and mass of the impurity are different from the force constant and the masses of the host lattice. The

[29] J. A. D. Matthew, Solid State Commun. 3, 365 (1965).

[30] For a complete list of references on this lattice defect problem see A. A. Maradudin, E. W. Montroll, and G. H. Weiss, in *Theory of Lattice Dynamics in the Harmonic Approximation*, edited by F. Seitz and D. Turnbull (Academic Press Inc., New York, 1963), Solid State Physics Suppl. 3.

long-range interaction forces which would introduce coupling between the different components of motion are not included. For the special case where the central and noncentral force constants of the host crystal are set equal to each other, three types of vibrational modes are associated with the impurity and its nearest neighbors. The three kinds of modes transform as the A_{2u}, (A_{1g} and E_g), and B_{2u} representations of the D_{4h} symmetry group.

Mitani and Takeno (MT)[28] have investigated the problem of local modes and gap modes for a substitutional defect in a diatomic simple cubic lattice of the NaCl type with host-ion masses M_1 and M_2. By using the M* coordinate developed by Maradudin *et al.*,[31] MT have reduced the equations of motion to a set of equations which are identical with those for a monatomic lattice which has a frequency-dependent mass M^*. A relatively simple equation for the eigenfrequency of the infrared-active A_{2u} mode can be obtained only if central and noncentral force constants are set equal to each other. Using the MT results, we now show that the equation giving the eigenfrequency for the A_{2u} mode can be cast into the simple form usually associated with the isotopic-mass-defect problem.

Mitani and Takeno show that if an impurity atom with mass M_1' and nearest-neighbor force constant K' replaces a host atom M_1, the following equation for the eigenfrequency of the infrared-active impurity mode is found:

$$1+\lambda-(\lambda+\epsilon)M_1\omega^2\Delta G(\omega^2;0,0,0) +\lambda(1-\epsilon)M_1\omega^2 G(\omega^2;1,0,0)=0, \quad \text{(A1)}$$

where

$$\lambda=(K'-K)/K, \quad \epsilon=(M_1-M_1')/M_1,$$

and

$$\Delta=\frac{\omega_1}{\omega_2}\left[\frac{(\omega/\omega_1)^2-(\omega_2/\omega_1)^2}{(\omega/\omega_1)^2-1}\right]^{1/2},$$

with

$$\omega_1^2=6K/M_1, \quad \omega_2^2=6K/M_2,$$

and $\omega_1<\omega_2$ for $M_1>M_2$. The Green's function is defined as

$$G(\omega^2;l_1,l_2,l_3)=\frac{1}{N}\sum_{k_1,k_2,k_3}\frac{\exp\{i(k_1l_1+k_2l_2+k_3l_3)\}}{M^*\omega^2-M^*\omega^2(\mathbf{k})},$$

where

$$M^*\omega^2=6K\{[(\omega^2/\omega_1^2-1)(\omega^2/\omega_2^2-1)]^{1/2}+1\}$$

and

$$M^*\omega^2(\mathbf{k})=2K(3-\cos k_1-\cos k_2-\cos k_3),$$

where N is the number of atoms in the lattice, K is the force constant for the perfect lattice, $\mathbf{k}=(k_1,k_2,k_3)$ is the wave vector, and the lattice constant is taken as unity. The set of integers specifying lattice sites are (l_1,l_2,l_3) and the sum extends over the first Brillouin zone. Equation (A1) can be expressed in terms of only one Green's function by using the following identity relation given by MT:

$$(M^*\omega^2-6K)G(\omega^2;l_1,l_2,l_3)+K[G(\omega^2;l_1-1,l_2,l_3) +G(\omega^2,l_1+1,l_2,l_3)+G(\omega^2;l_1,l_2-1,l_3)+G(\omega^2;l_1,l_2+1,l_3) +G(\omega^2;l_1,l_2,l_3-1)+G(\omega^2;l_1,l_2,l_3+1)] =\delta(l_1)\delta(l_2)\delta(l_3). \quad \text{(A2)}$$

We find that

$$6KG(\omega^2;1,0,0)=1-[(\omega^2/\omega_1^2-1)(\omega^2/\omega_2^2-1)]^{1/2} \times 6KG(\omega^2;0,0,0). \quad \text{(A3)}$$

Substituting Eq. (A3) into (A1), the eigenfrequency of the A_{2u} local mode is given by the solution of

$$1+\lambda+\lambda(1-\epsilon)(\omega/\omega_1)^2-\{\epsilon(1+\lambda)+\lambda(1-\epsilon)(\omega/\omega_1)^2\} \times(\omega/\omega_1)^2 6K\Delta G(\omega^2;0,0,0)=0, \quad \text{(A4)}$$

which has the desired form of

$$y^2B(y)=1/\epsilon^*, \quad \text{(A5)}$$

where $y=\omega/\omega_1$,

$$\frac{1}{\epsilon^*}=\frac{1+\lambda+\lambda(1-\epsilon)y^2}{\epsilon(1+\lambda)+\lambda(1-\epsilon)y^2}, \quad \text{(A6)}$$

and

$$B(y)=6K\Delta G(\omega^2;0,0,0). \quad \text{(A7)}$$

For the special isotopic defect where $K'=K$, it is found that $\lambda=0$ and

$$1/\epsilon^*=1/\epsilon,$$

and Eq. (A5) reduces to

$$y^2B(y)=1/\epsilon,$$

which is the well-known expression for the eigenfrequency of the mass-defect local mode.[7]

For the particular problem of gap modes, we now restrict Eq. (A5) to the frequency region where $\omega_1\leq\omega\leq\omega_2$. The values of $G(\omega^2;0,0,0)$ for this frequency region have been tabulated (Table I)[28] by MT. Using their table, our calculated $y^2B(y)$ is shown graphically in Fig. 7.

[31] A. A. Maradudin, P. Mazur, E. W. Montroll, and G. H. Weiss, Rev. Mod. Phys. **30**, 175 (1958).